Simulating Urban Satellite-Based Vehicular Networks: Focus on Maps, Building Heights, or Vehicle Density?

Enrico Zanotto, Leonardo Maccari
Dept. of Environmental Sciences, Informatics and Statistics
Ca' Foscari University of Venice
Venice, Italy
887566@stud.unive.it, leonardo.maccari@unive.it

***Abstract*—Low-Earth Orbit constellations are one of the recent advancements that could provide a fresh perspective on Internet connectivity. They are appealing because they provide global coverage, they offer low round-trip-time, and they can grow to tens of thousands satellites to increase the offered capacity. However, simulating large urban areas is challenging due to the scalability limitations of the simulators. We present the results of a simulation campaign in which we improve the current state-of-the-art vehicular network simulator, Veins, in its satellite-based variant (Space Veins). We introduce a precise three-dimensional analysis that allows us to use detailed city maps, which in turn allows us to use realistic traffic patterns. We show that the parameters that most impact the results of the simulators are two: the assumptions on the building height and the positioning of the vehicles in the map. Results are extremely sensitive to these factors, underscoring the need for more open data and standardized, repeatable scenarios that can facilitate better research evaluation in this field.**

I. Introduction

Over the last decade the cost of space launches per kg of payload has steeply decreased, and as a consequence, the number of satellites skyrocketed. One killer application is of course telecommunications, with several operators that already launched their constellation of *Low-Earth-Orbit* (LEO) satellites to offer network connectivity. Starlink is probably the most developed one (with thousands of active satellites) and Iridium is one of the most known and studied [1]. The fast advancement of LEO constellations have led researchers to analyse the possibility of connecting mobile terminals directly to the satellite infrastructure. The current proposals plan to exploit mmWave frequencies (from 30 to 300 GHz) in order to provide enough capacity [2], but that comes with many challenges. Among them, we need scalable and accurate tools to design and assess the performance of satellite connectivity. We can exploit theoretical models to estimate upper and lower bounds, we can leverage on experimental evaluation for link-level measurement, however, when we need sufficiently detailed evaluation together with scalability, network simulators play a fundamental role.

Recently, some works have integrated satellite constellations into vehicular network simulators [3]. The challenge with this approach is to simulate large-scale urban areas with hundreds of thousands of vehicles and tens of satellites offering connectivity in a certain area. Given the multitude of parameters to study (location of the vehicles, latitude/longitude of the scenario, accuracy of the simulation map) it is important to use models that provide a good trade-off between accuracy and performance, but it is absolutely not trivial to set the bar on the level of detail needed to retain realistic results. The goal of this paper is to showcase that merging very recent approaches for vehicular network simulators, we are able to study satellite coverage in realistic three-dimensional (3d) scenarios with a precise calculation of the presence of *Line-Of-Sight* (LOS). We focus on the evaluation of LOS because at high frequencies, it is very unlikely to use *Non Line-Of-Sight* (NLOS) links, and even if possible, the performance is strongly penalized [4].

Our approach consists of three steps: i) we run a vehicular simulation in order to sample the density of vehicles per square meter, in a real city map; ii) we reproduce the 3d scenario using open data that describe the city map and the building height, and we place static vehicles based on the density previously estimated; iii) we run a 24h simulation using the orbits of the Iridium network.

Our results show that each of these steps has a relevant impact on the results, and simple configurations like a Manhattan grid leads to results that are far from those obtained with more realistic assumptions.

II. State of The Art

Using non-terrestrial networks to connect mobile devices is a topic that has raised the interest of researchers, as it would ensure an ubiquitous connectivity for mobile phones and vehicles in urban and non-urban areas. In particular, the idea of integrating non-terrestrial networks using mmWave in 6G has been explored because it can provide high capacity to moving devices [5], [2]. The telecommunication challenges are however non trivial at all, because NLOS communication is almost impossible in the highest portion of the mmWave spectrum. This calls for a very high density of satellites or the possible adoption of relays (*High Altitude Platform*s (HAPs) or drones) that repeat the signal towards the vehicles. How-

ever, this kind of infrastructure is extremely challenging to design [6] so it is very important to estimate the availability of LOS from LEO satellites to vehicles directly.

This task can be approached using several techniques, on the one extreme some works use an analytical approach [7], [8], that is very useful to assess the macroscopic properties of the system, but of course lack the granularity that is required to design and optimize a real network. On the other extreme we have experimental works that use real networks to measure their performance [9]. These papers are valuable to model the performance of communication links but are very expensive to realize, so their scale is intrinsically limited. Moreover, they can only use available infrastructure and thus they can not be used to test non existing network set-ups. A middle approach is the simulation-based one, that exploits the models produced by theoretical and experimental works, and it can be tailored to the scale and the scenario that the researcher wants to explore.

Not many works have explored the feasibility of non-terrestrial connectivity for vehicular networks. Initial works by Franke et al. have addressed the feasibility of simulating satellite-based vehicular networks [3] and introduced realistic datalink layer strategies [10]. More advanced works by the same authors improved the open source simulators[1] to introduce real satellite trajectories and accurate geometric approximations to map satellite orbits to the local projection used in the simulator [11]. On this basis the availability of LOS in simplified city models was studied, making an initial estimation of the impact of the geometry of the urban environment on the vehicle connectivity [12]. The scarcity of results is in part due to the fact that vehicular network simulators use statistical path loss models that are not tailored to mmWave communications. In mmWave communications the impact of LOS/NLOS, and eventually diffraction requires a precise 3d modelling of the scenario. However there is a lack of data and software to correctly model 3d vehicular networks [13], and ray-tracers are computationally expensive [14]. A similar problem has been addressed recently for 5G connectivity [15], [4] and led to the release of new, up-to-date algorithms that can be efficiently used to simulate detailed 3d scenarios in urban vehicular networks without incurring in the computing overhead introduced by classical ray-tracing simulators [16].

This paper pushes forward the state of the art merging three approaches: the simulator tools by Franke et al. [12], the LOS estimation by Zanotto et al. [16], and the density-based approach by Gemmi et al [4] for an accurate positioning of vehicles. We exploit precise models for the satellite orbits, and we represent an urban area with a detailed, realistic, 3d scenario, to efficiently compute the presence of LOS with a scalable approach[2]. Our results confirm a strong dependency on the building heights and highlight the importance of vehicle density, that can be derived only using realistic traffic patterns.

[1]See https://sat.car2x.org/

[2]Our code is available at: https://github.com/UniVe-NeDS-Lab/space_veins/tree/space_veins_3d

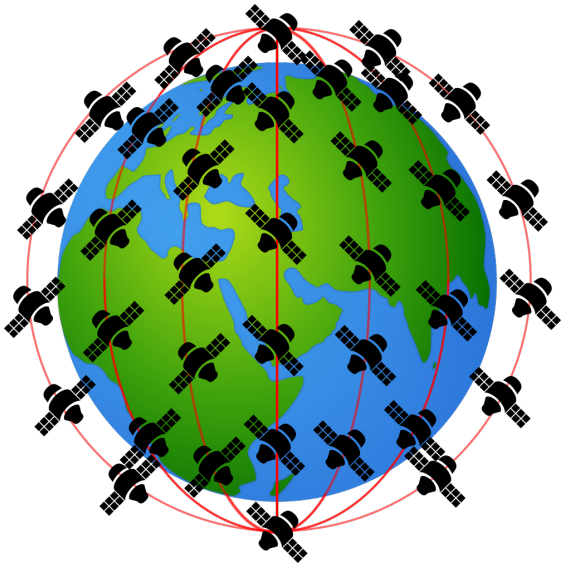

Fig. 1: A pictorial representation of the Iridium Next constellation.

III. Simulation Set-Up

We divide the scenario description in two parts, the satellite network and the ground devices. We base the analysis on the Iridium Next constellation, that is well documented [1], and its integration in OMNet++ is thoroughly discussed in [11]. Here we provide only the details that are relevant for our analysis.

A. The Satellite Network

A LEO constellation is a set of satellites orbiting around the globe, at an altitude in the order of hundreds of kilometers. With such a low altitude the satellites complete a whole orbit in roughly 90-100 minutes, which means that satellites travel at a speed of tens of thousands of km per hour. Besides the altitude, a LEO satellite orbit is defined using an inclination angle, that is the angle of the orbit plane with reference to the equator plane. Iridium currently uses a constellation of 75 satellites at an altitude of 780km, with a nearly polar orbit, which means that the inclination is 86.4°, close to the inclination of a meridian. Satellites then pass close to the north and south pole, which means that coverage can be provided even in regions with an extreme latitude.

As shown in Fig. 1, the 75 satellites are distributed over 6 orbits spaced 30° each[3]. Satellite orbits are defined by a so-called *Two-Line Element Set* (TLE), that contains all the data that are needed to reconstruct the orbit. For each satellite, its TLE can be downloaded by observation websites[4].

[3]Note that not all the constellation is used all the times, as 5 satellites are left as a spare backup, but we include them in our simulation for completeness.

[4]http://celestrak.org/NORAD/elements/gp.php?GROUP=iridium-NEXT\&FORMAT=tle

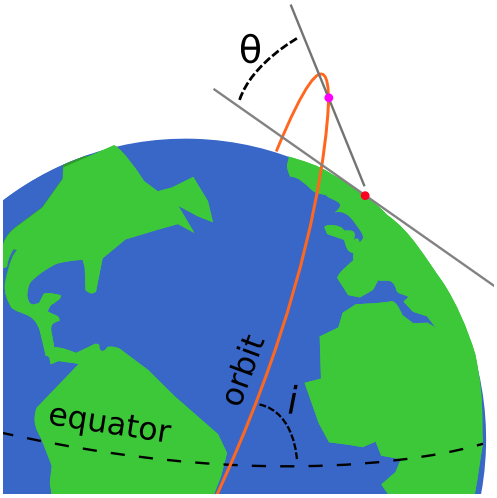

Fig. 2: A pictorial representation of an orbit to illustrate its geometry. Dashed line: equator, orange line: orbit, red dot: receiver, purple dot: satellite position. i is the inclination angle and θ the elevation angle

.

Satellites can communicate with ground terminals directly. The communication link has a different length depending on the elevation angle θ: the angle formed by the segment representing the communication link and the plane tangent to the earth surface (see Fig. 2). If $\theta = 90°$ then the satellite is exactly at the Zenith of the observer point, in absence of obstacles, the lowest angle that Iridium allows for communications is $8.2°$ [1].

Given these constraints, one ground terminal remains in LOS with a satellite for only a few minutes and needs to hand-over the communication frequently. Iridium does not use mmWave communication with ground terminals, however, our goal is not to study a specific communication network, it is to verify what are the factors that impact the most the simulation of a satellite network. We then use Iridium as an example of a realistic network deployment, but the same experiments could be repeated with other constellations, such as Starlink.

Note that since the orbit period is lower than the earth revolution period, when an orbit is completed, the satellite finds itself on the Zenith of a different ground point compared to the previous passage. Since the earth revolution period is not a precise multiple of the orbit duration, after 24 hours the satellite finds itself on the Zenith of yet another ground point. This means that even after 24 hours the state of the simulation is not the initial one, so the configuration of satellites did not explore all the possible states. In this work we stop the simulation after 24 hours for practical reasons.

B. The Ground Network

We simulate two scenarios in the terrestrial part of the network, in both cases we placed static vehicles on the streets. The first one is a classical Manhattan grid scenario with buildings of height 10m, 16.2m, 30m, that we refer to as M-10/16/30 (16.2m is the average height of the buildings in the Luxembourg scenario that we describe next). We use an area of roughly one square km with a target density of 100 cars per square km distributed with a deterministic algorithm that places cars at regular intervals along the streets, that is the basic strategy adopted in other papers [12]. The center of the area is placed at the same latitude and longitude of the center of the scenario we describe next.

The second scenario is extracted from Luxembourg city (we refer to it as Lux). We use Luxembourg due to the availability of accurate data, that increases the realism of our results. First, Veins/SUMO can be integrated with the LuST traffic generator, that uses a highly realistic synthetically generated traffic demand, validated using the traffic traces measured in site [17]. Second, we obtained the precise description of the 3d representation of the city (the so-called *Digital Surface Model* (DSM)) that enables us to reproduce the city buildings with great accuracy. In Lux we use the real map of the city extracted from OpenStreetMap, the building shapes and their real height. We approximate the buildings to prisms and we admit both convex and concave prisms, thanks to the techniques introduced in a previous work [16]. This is the first time in our best knowledge that a precise 3d simulator is used to study a satellite-based vehicular network.

When using Lux we could simulate a network with moving vehicles, but this has high scalability problems. Even if the area under analysis is relatively small (we select a rectangle of 1.46 square km, that corresponds to a neighborhood of the city delimited by avenues), the traffic patterns have sources and sinks of vehicles outside the area we select. So we would still need to simulate a city-wide area with hundreds of thousands of cars plus all the satellites. Another issue with this approach is that we could hardly compare it with the Manhattan scenario that would have completely synthetic and regular traffic patterns.

We then decided to use an approach that has been already successfully used in similar works [15], [4]. We run a 24h simulation of only the vehicular traffic in the Luxembourg scenario, without considering any communication (involving more than 200,000 cars). At every second we sample the position of the vehicles, and we quantize the samples using units of one square meter. We then have two integer indices $0 \leq x \leq X$ and $0 \leq y \leq Y$ where $X \times Y$ is the size of the area. We obtain a matrix $\boldsymbol{\gamma}$ where $\boldsymbol{\gamma}_{x,y} = n$ means that n vehicles have passed in cell (x, y) during the whole simulation. We refer to n as the number of *samples* per point and we call G the set of all coordinates where at least one sample was measured:

$$G = \{(x, y) \text{ s.t. } \boldsymbol{\gamma}_{x,y} \neq 0\} \tag{1}$$

Based on this initial data we distribute the vehicles, downsampling the space to reduce the complexity. Given a target density of vehicles per square km D, we tessellate the 2d space with a number $r \times q$ of squares so that we have D squares per square km, each one identified with two indices $i \in [0, r-1], j \in [0, q-1]$. We create $\boldsymbol{\gamma}^{i,j}$ that is a

submatrix of γ restricted to the coordinates (x, y) that fall in the square identified by indices i, j, we call $G_{i,j} \subseteq G$ the subset of coordinates in the square. Note that not all the squares contain valid points, as some can be entirely included in buildings, we call $R \leq rq$ the number of sets $G_{i,j}$ with non-zero size. We now need strategies to choose (on average) one point in each $G_{i,j}$, so that the chosen point(s) can be considered somehow representative of square i, j.

1) Uniform Downsampling Strategies: In the first downsampling strategy (which we refer to as the uniform strategy), for each couple i, j we just select the point in $G_{i,j}$ whose distance to the center of the square (computed as the intersection of its diagonals) is minimal. This strategy produces coordinates that are spread uniformly in the 2d space but are not representative of the density of vehicles. Moreover, we can not guarantee a certain density D as $R \leq rq$. Fig. 3 reports the distribution of the receivers in the simulation using the uniform placement. The grid determines the number of squares, the grayed out squares are the ones that contain no samples, the color gamma represents $\gamma_{x,y}$. We see that the range of samples is limited to about 1000 samples per point, and most of the points are in the low region of the gamma.

Fig. 3: Uniform placement. The points are distributed uniformly to cover the largest portion of the area, but the samples per point are very low.

We need a second strategy that, given two coordinates couples x_1, y_1 and x_2, y_2 so that $\gamma_{x_1,y_1} > \gamma_{x_2,y_2}$ selects x_1, y_1 with higher probability.

2) Weighted Downsampling Strategy: We could simply use the points in the area with the highest $\gamma_{x,y}$, however when using a realistic traffic pattern, we know that the distribution of $\gamma_{x,y}$ is very skewed. The average is less then one sample per minute, but top values are orders of magnitude higher than the average and are all concentrated on crossroads with a high vehicular traffic [4]. Choosing the top-R coordinates based on the number of samples would generate a set of positions that are all concentrated in a few locations.

In the second strategy (which we refer to as the weighted strategy) we then operate as follows. We call $s = |\gamma|$ and $s_{i,j} = |\gamma^{i,j}|$ (where $|\cdot|$ is the sum of all the elements of the matrix). Given R we computed in the uniform placement strategy, for every submatrix we compute

$$g_{i,j} = \lfloor R \frac{s_{i,j}}{s} \rfloor \quad (2)$$

$$r_{i,j} = R \frac{s_{i,j}}{s} - g_{i,j} \quad (3)$$

Where $g_{i,j}$ is R scaled by the ratio between the sum of the samples measured in block i, j and the total number of samples, rounded to the lowest integer. Instead, $r_{i,j}$ is the residual difference with the floating point value. Note that $g_{i,j}$ can be larger than one, and due to the rounding, $g_{i,j}$ can be also zero, so $\sum_i \sum_j g_{i,j} = R' \leq R$.

We take the list $L = \{g_{i,j} \ \forall \ (i,j) \,|\, g_{i,j} \neq 0\}$ and then for each block $(i, j) \in L$ we take $g_{i,j}$ coordinates starting from the ones with the highest number of samples. This will assign R' coordinates to $S \leq R'$ squares. If $R' < R$ we order the blocks by decreasing values of $r_{i,j}$ and assign the remaining $R - R'$ points, one per square. This strategy can provide any given density D of points, however, in order to compare the absolute values of the performance metrics, we use the same number of coordinates R generated by the uniform strategy.

As a comparison, Fig. 4 shows the same area we used for Fig. 3 on which we applied the weighted sampling. The choice clearly covers a smaller area, but each point is associated with a larger number of samples (note that the color map is the same, but the gamma extremes are 50 times larger than in Fig. 3). In practical terms this means that the coordinates chosen with the weighted algorithm are less representative in terms of space density, but are way more representative of the probability of having a vehicle in that position.

Fig. 4: Weighted placement. The covered area is smaller, but the samples per point are one order of magnitude higher.

In the area under analysis (1.46 square km) we pick a density $D = 70$, that creates a tessellation made of 112 squares (higher than 70*1.46 due to border conditions). The properties of the sampled points are reported in Tab. I, where we report the number of chosen coordinates, the number of occupied squares and the percentage of the occupied squares with reference to the non-empty squares. We can see that

strategy	R	occupied squares	non-empty squares (%)
uniform	106	106	100%
top-R	106	18	16.1%
weighted	106	59	52.7%

TABLE I: The properties of the sampled coordinates set.

given a certain target density, we obtain the number of non-empty square from the first strategy, that corresponds to all the squares that have at least one coordinate in it. The top-R strategy will distribute the coordinates in only 18 of the 106 available squares, while the weighted strategy occupies 59 squares.

Note that the use of static vehicles with a downsampling strategy has another advantage we can exploit in the future, as we could remove the whole simulator from the loop and replace it with a GPU. In fact the positions of the satellites are deterministic and given, and the positions of the vehicles are static. We could extract the data from one simulator run and then use the power of parallelisation offered by a GPU to compute the presence of LOS in areas that are otherwise impossible to simulate due to their size.

IV. The Evaluation Metrics

Every second, every satellite sends a broadcast packet that is potentially received by all the vehicles. The channel model simply computes the segment line between the sender and the receiver, checks if this segment intersects any of the buildings in the 3d scenario and verifies the presence or absence of LOS. If LOS is present we consider the frame delivered, else we consider it not delivered. When the elevation of the satellite with reference to the vehicle position is below 8.2° the frame is never delivered. At the end of the evaluation the simulator produces a comma-separated-values file that contains for each receiver a line of log for each frame, including the position of the receiver, the availability of LOS, the elevation angle of the satellite with reference to the vehicle position, and the distance. We set the number of vehicles to 100 on every scenario in order to have comparable absolute numbers.

To evaluate the results of the simulation we use several evaluation metrics. The first one is the fraction of frames F that were delivered using LOS over the total sent frames, measured in each receiving vehicle. We compute F_v for each vehicle v and we report the empirical distribution of this value. For each delivered frame we save the elevation angle θ of the satellite that generates the frame, computed with reference to the vehicle position. This is obviously affected by the geometry of the scenario, by the height of the buildings and by the positions of the vehicles. It is extremely important because it determines the length d of the link from the satellite to the vehicle. The value of d depends on $sin(\theta)$ and thus the distance is non linear with θ. On top of this we also know that the expected capacity of the link depends non-linearly on d. In order to clearly show the impact of θ we then compute the Shannon capacity of the link used to deliver the frame, similarly to Giordani et al. [5]. The exact equations and parameters are reported in Appendix A. We show the distribution of the Shannon capacity as a binned histogram.

Before moving to the results let us summarize the goals of the evaluation: we can group the scenarios in 3 sets: M10 and M30 that require only synthetic data; M-16 that uses an estimation of the average building height; Lux-U that requires the real city map and the real building heights; Lux-W that requires also accurate traffic patterns. For the Manhattan scenarios, LOS is computed with simple techniques, because the obstacles are convex ones. For the Lux scenario (and any other real-world 3d scenario) we need a more robust 3d ray-tracing techniques as the one in Zanotto et al. [16], as the building bases can be concave. Every step increases the complexity of the simulator and we want to evaluate what is the impact on the results. As both the vehicles positions and satellite trajectories are deterministic, we show the results of one single run that lasts 24 hours.

V. Results

A. Fraction F of LOS Frames

The first results we present show the fraction of LOS frames that are received by the vehicles. Fig. 5 shows the sorted values of F_v, for all the scenarios. We can clearly see that Manhattan scenarios are strongly influenced by the choice of the building height, which is a sensitive parameter. This confirms previous results with similar settings [12]. We also notice that the road grid introduces a synthetic clustering of the data, with vehicles that are distributed in the same direction, or the same street, that behave in a similar way. Some of the vehicles (the ones that are placed in a crossroad) have a higher visibility. It is intuitive to understand that since Iridium orbits are almost polar, the streets that have a North-South orientation have a better coverage than ones with East-West orientation. In principle, the same effects exists also in the Luxembourg scenario, but streets are not on a grid, so the distribution of F_v is smooth and does not have sharp steps. We also notice that the Lux-W curve has significantly better performance than the Lux-U. This is a key observation of our results: *uniform 2D sampling strongly underestimates the performance of the system, compared to weighted sampling*. We will give an intuitive explanation in Section VI.

We also summarize the distribution of F with box-plots, shown in Fig. 6. We see that the decrease in the median of the three Manhattan scenarios is almost the same (0.14 between M-10 and M-16 and 0.13 between M-16 and M30), even if the building height is not linearly increasing, as the first interval is 6.2m and the second is 13.8m. This can be explained because the portion of sky that one point in the street can see without obstruction doesn't reduce linearly with the building height, so there is a threshold effect that could be captured with a denser sampling of the buildings height. From these results we can draw three conclusions: i) Manhattan scenarios are sensitive to the building heights, especially in the low heights range; ii) a periodic road topology (like a grid) introduces an artificial clustering effect;

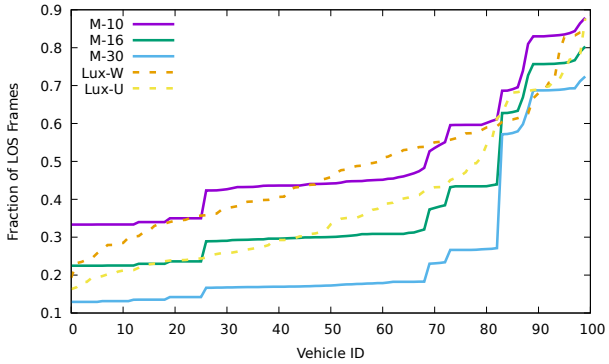

Fig. 5: The sorted values of the fraction of frames received in LOS (F_v) in all scenarios.

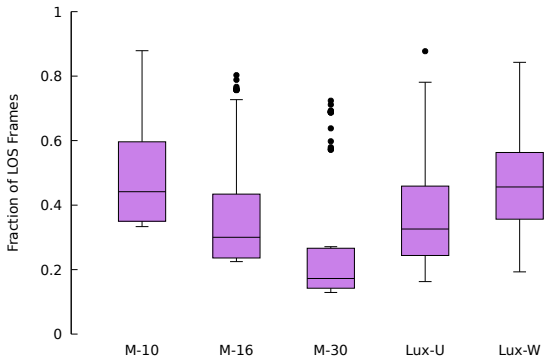

Fig. 6: The boxplots summarising the distribution of F_v in all the scenarios.

iii) when using an accurate 3d topology, the distribution of vehicles has a strong impact on the final results.

B. Elevation Angle θ

We first illustrate in an intuitive way the measured values of the elevation θ, to visualize the peculiarity of the satellite network. Fig. 7 reports 260 minutes of the M-16 scenario, and shows that the performance of the satellite network oscillate with two periods. The first is $\alpha \simeq 8min$ that represents the time between the passage of two satellites belonging to the same orbit over the simulation area. We see that in the Iridium constellation the satellites in one orbit are not dense enough to avoid a huge oscillation of the angle when the receiver passes from one satellite to the other. If the density was higher the angle would be the convolution of more curves with a lower fluctuation. The second period $\beta \simeq 120min$ is the time difference between two separate orbits, that is consistent with having 6 orbits that split the 24 hours in 12 passages per day. We notice that the descending part of one curve has a small overlapping with the ascending part of the next one, confirming that the density of Iridium is not sufficient to avoid strong fluctuations.

Fig. 8 reports the distribution of θ binned on intervals of 10°, for all the scenarios. There are several relevant things to note. The first one is that the curves for the Manhattan

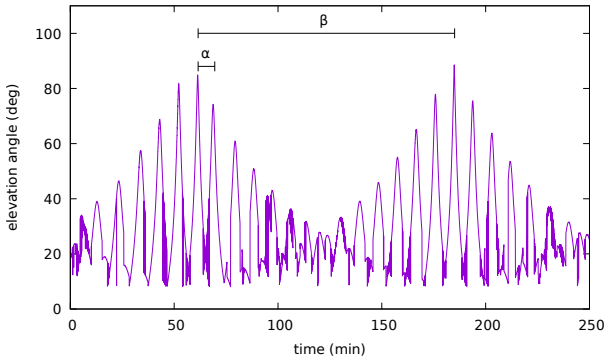

Fig. 7: The angle θ measured on LOS links over 260 minutes simulation in the M-16 scenario. Data are smoothed with a moving average of 10 minutes and downsampled for readability.

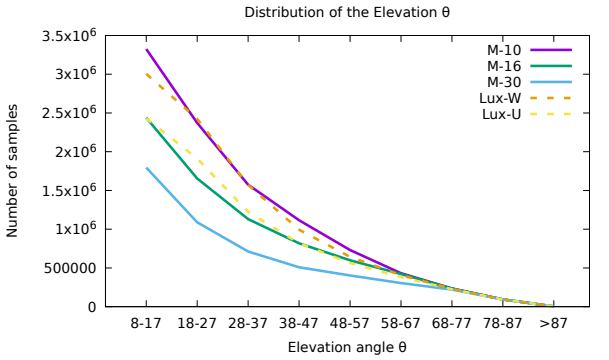

Fig. 8: The angle θ measured on LOS links over a 24h simulation in all the tested scenarios.

scenarios are well separated, that confirms that the building heights is a very sensitive parameter. The second is that the Manhattan scenario with building heights 16.2 has a performance that is close to the Luxembourg scenario with uniform distribution of vehicles. However, when we consider the Luxembourg scenario with the weighted distribution of vehicles, we see that the difference is again, very relevant. This suggests that to have realistic results for a specific urban area, the building heights and the vehicles distribution have a stronger influence than the city map.

C. Link Capacity

Finally we present the results on the estimated link capacity, that is reported in Fig. 9. Here we can make three key observations: the first one is that the distributions have a similar shape, meaning that the factor that mostly influences it is the latitude of the urban area and the geometry of the constellation, rather than the topological properties of the urban area. However, the curve in the Lux scenarios is more compact and skewed, as the mode of the distribution is shifted right and the tail of the distribution is more steep. This is pretty evident when comparing the Lux-U with the M-16 curves, that cross each other twice.

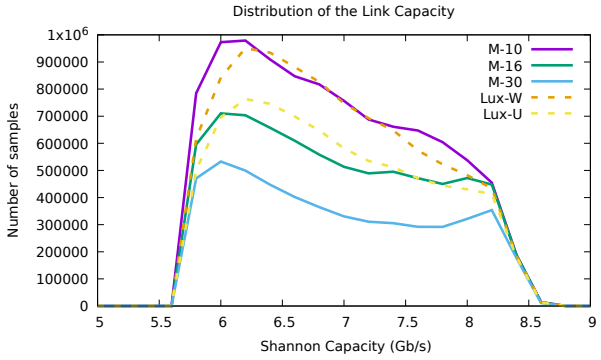

Fig. 9: The Shannon capacity estimated on LOS links over a 24h simulation in all the tested scenarios.

VI. Discussion and Limitations

The results we presented must be translated into practical advice for the researchers that use simulation tools to study the performance of LEO communications in the mmWave bandwidth:

The Building Heights Must Be Accurate: The results are very sensitive to the building height, so that accurate data for the urban area under analysis is of paramount importance. Unfortunately, open data of buildings height are scarce, and thus, *there is a need to estimate and produce more open data that researchers can use to set-up accurate 3d representations of urban and non urban areas*.

The City Map Influences the Distribution of F_v but not the Median: If the average value of the building heights is given and the distribution of vehicles is uniform, then the median of F_v for the Manhattan scenario is close to the realistic one. However, the Manhattan scenarios introduces non realistic clustering and distorts the curve of the link capacity.

The Vehicles Distribution has a Strong Impact: When vehicles are placed following a data-derived distribution the results are strikingly different than when the placement is uniform. Uniform placement underestimates performance: *we need more open data to create realistic and repeatable vehicular networks scenarios*.

The last point is a key one that deserves a deeper analysis. An intuitive explanation is that using a weighted sampling we introduce a bias towards streets that have higher traffic, and those streets are probably larger than ones where the traffic is lower. As a consequence, the buildings are farther away from the vehicles, and the vehicles have a better sky visibility. This increases the probability of being in LOS with a satellite. However, if we compare the Lux curves in Fig. 8 and Fig. 9 we see that the largest difference is for the smaller angles and smaller capacity. This is compatible with our intuition: vehicles that are placed in high-traffic streets have a larger visibility, and thus, they have LOS with satellites that have a lower elevation θ, but this implies links with lower capacity. This information is fundamental for the use of relays, such as HAPs [18], or drones, that are one key component to the success of satellite networks. A HAP can be used as a repeater between a satellite and the user terminal when there is no direct LOS: our results suggest that counterintuitively, HAPs should not be placed where there is a high density of vehicles as these are the areas in which F tends to be higher. It might then be more convenient to use HAPs in areas with lower vehicles density, and lower average LOS. One way to approach this problem would be to compute some spatial centrality metric that takes into account the traffic density, and choose the HAPs positions in order to maximise their overall centrality. Centrality metrics have been used in graph analysis and routing [19], [20] and can be adjusted for many purposes.

One limitation of this approach is that we are considering the average behavior represented by a static snapshot of the vehicle positions. This intrinsically hides the dynamic behavior of the system. For instance, we don't know what is F computed on an *average trajectory* inside the urban area, if it shows a certain continuity or it is subject to large periods of service interruption. However, we have the data of the original vehicle trajectories, and without changing our approach we could model how the simulation parameters affect the coverage of trajectories, and not of single points.

VII. Conclusions

The focus of this paper is on the identification of the most important parameters that influence large-scale simulations of LEO networks for vehicle connectivity. We compare three simulation approaches, the simplest one based on a grid topology, a second one based on an accurate 3d topology and uniform vehicles placement, and a third one that improves the second with a realistic placement of vehicles based on traffic traces. We show that as long as the vehicles are placed uniformly in the road networks, a Manhattan scenario using the average building heights has a median behavior that is similar to the one measured on the realistic scenario. However, when vehicles positions are chosen based on the realistic traffic patterns, the results change completely. Simulations must be then tailored to the specific urban area, and need highly detailed data about the building heights and the vehicle density.

References

[1] S. R. Pratt, R. A. Raines, C. E. Fossa, and M. A. Temple, "An operational and performance overview of the IRIDIUM low earth orbit satellite system," *IEEE Communications Surveys*, vol. 2, no. 2, 1999.

[2] M. Giordani and M. Zorzi, "Non-terrestrial networks in the 6g era: Challenges and opportunities," *IEEE Network*, vol. 35, no. 2, 2021.

[3] M. Franke, F. Klingler, and C. Sommer, "Poster: Simulating Hybrid LEO Satellite and V2X Networks," in *2021 IEEE Vehicular Networking Conference (VNC)*, Nov. 2021.

[4] G. Gemmi, M. Segata, and L. Maccari, "Estimating coverage and capacity of high frequency mobile networks in ultradense urban areas," *Computer Communications*, vol. 223, 2024.

[5] M. Giordani and M. Zorzi, "satellite communication at millimeter waves: a key enabler of the 6g era," in *2020 International Conference on Computing, Networking and Communications (ICNC)*.

[6] A. Traspadini, M. Giordani, and M. Zorzi, "UAV/HAP-Assisted Vehicular Edge Computing in 6G: Where and What to Offload?" in *2022 Joint European Conference on Networks and Communications & 6G Summit (EuCNC/6G Summit)*, Jun. 2022.

[7] H. Wu, M. He, X. Shen, W. Zhuang, N.-D. Dao, and W. Shi, "Network Performance Analysis of Satellite–Terrestrial Vehicular Network," *IEEE Internet of Things Journal*, vol. 11, no. 9, May 2024.
[8] A. Al-Hourani, "Line-of-Sight Probability and Holding Distance in Non-Terrestrial Networks," *IEEE Communications Letters*, vol. 28, no. 3, Mar. 2024.
[9] A. Yastrebova-Castillo, M. Höyhtyä, M. Majanen, T. Ojanperä, J. Scholliers, and S. J. Rantala, "Improving the safety of autonomous driving by using Direct-to-Satellite connectivity: the case of Iridium and Starlink satellite constellations," in *2023 IEEE Conference on Standards for Communications and Networking (CSCN)*, Nov. 2023.
[10] M. Franke, F. Klingler, and C. Sommer, "Addressing the Unbounded Latency of Best-Effort Device-to-Device Communication with Low Earth Orbit Satellite Support," in *2023 IEEE 20th Consumer Communications & Networking Conference (CCNC)*, Jan. 2023.
[11] M. Franke and C. Sommer, "Toward Space-Air-Ground Integrated Network Simulation with 4D Topologies," in *Wireless On-Demand Network Systems and Services Conference (WONS)*, 2024.
[12] ——, "Obstacle Shadowing in Vehicle-to-Satellite Communication: Impact of Location, Street Layout, Building Height, and LEO Satellite Constellation," in *IEEE Vehicular Networking Conference (VNC)*, 2024.
[13] A. Brummer, R. German, and A. Djanatliev, "Methodology and Performance Assessment of Three-Dimensional Vehicular Ad-hoc Network Simulation," *IEEE Access*, vol. 11, 2023.
[14] E. Egea-Lopez, J. M. Molina-Garcia-Pardo, M. Lienard, and P. Degauque, "Opal: An open source ray-tracing propagation simulator for electromagnetic characterization," *PLOS ONE*, vol. 16, no. 11, 2021.
[15] G. Gemmi, M. Segata, and L. Maccari, "Vehicles or pedestrians: On the gNB placement in ultradense urban areas," in *18th Wireless On-Demand Network Systems and Services Conference (WONS)*, 2023.
[16] E. Zanotto and L. Maccari, "Evaluating the Impact of a 3D Simulation Model on the Performance of Vehicular Networks," in *Wireless On-Demand Network Systems and Services Conference (WONS)*, 2024.
[17] L. Codeca, R. Frank, S. Faye, and T. Engel, "Luxembourg sumo traffic (lust) scenario: Traffic demand evaluation," *IEEE Intelligent Transportation Systems Magazine*, vol. 9, no. 2, 2017.
[18] G. Karabulut Kurt, M. G. Khoshkholgh, S. Alfattani, A. Ibrahim, T. S. J. Darwish, M. S. Alam, H. Yanikomeroglu, and A. Yongacoglu, "A Vision and Framework for the High Altitude Platform Station (HAPS) Networks of the Future," *IEEE Communications Surveys & Tutorials*, vol. 23, no. 2, 2021.
[19] L. Maccari and R. Lo Cigno, "Improving Routing Convergence with Centrality: Theory and Implementation of Pop-Routing," *IEEE Transactions on Networking*, vol. 26, pp. 2216–2229, Oct. 2018.
[20] L. Maccari, L. Ghiro, A. Guerrieri, A. Montresor, and R. Lo Cigno, "Exact Distributed Load Centrality Computation: Algorithms, Convergence, and Applications to DV Routing," *IEEE Transactions on Parallel and Distrbuted Systems*, vol. 31, pp. 1693–1706, July 2020.

name	meaning	value
N	Noise on the Receiver	(variable)
P_l	Path los	(variable)
C	Link Capacity	(variable)
k	Boltzmann Constant	1.380649×10^{-23}
T	temperature (K)	288
B	bandwidth	800MHz
f	frequency	28GHz
P_T	tx power	33 dBm
R_g	antenna gain at the receiver	50 dBi
T_g	antenna gain at the sender	43.2 dBi

TABLE II: Parameters used for capacity computation.

APPENDIX

Given the distance d, we use the classical Friis path loss estimation together with the Shannon equation using only the thermal noise as noise source. We adopt the parameters reported in Tab. II that are extracted from Giordani et al. [5]. As we are not interested to estimate the effective capacity, but to highlight the different estimation when using different simulation parameters, we don't include the effects of scintillation and atmospheric absorption. As a result, compared to Giordani et al. we measure a higher capacity. The path loss is computed using the free space path loss equation in decibel (Eq. (4)) and then plugged in the Friis equation (Eq. (5)) to obtain the received signal strength S. Thermal noise is computed as in Eq. (6) and used to compute the signal-to-noise ratio (after conversion of S in linear scale). Finally the Shannon equation is used to compute the capacity in bit/s Eq. (7).

$$P_l = 20log_{10}(d) + 20log_{10}(f) - 147.55 \quad (4)$$

$$S[dB] = P_T + T_g + R_g - P_l \quad (5)$$

$$N = k * T * B \quad (6)$$

$$C = Blog_{10}(1 + \frac{S}{N}) \quad (7)$$